A revised manuscript for publication in

Chemical Engineering Research and Design

On the Performance of a Spouted Bed Type Device for Feeding Spent Coffee Grounds to a Circulating Fluidized Bed Reactor

L. Massaro Sousa[1], and M. C. Ferreira[1*]

[1]Drying Center for Pastes, Suspensions, and Seeds, Chemical Engineering Department,

Federal University of São Carlos, P.O. Box 676, 13565-905 São Carlos, Brazil

*Corresponding author. mariaf@ufscar.br (M. C. Ferreira), lucas.massarosousa@gmail.com (L. Massaro Sousa).
CFB: circulating fluidized bed; SB: spouted bed; SCG: spent coffee ground; LV: L-valve.

1 Introduction

Spouted beds (SBs) provide effective contact between the fluid and solid phases within a fluidized vessel. This fluidization technique was first proposed by Mathur and Gishler (Mathur and Gishler, 1955) as an alternative to prevent slugging observed in fluidized beds of coarse particles. A general search in the Science Direct database shows that to date, more than 3,000 research papers have been published reporting the use of SBs in a wide variety of applications, including drying, coating, granulation and reaction operations (Cui and Grace, 2008; Jono et al., 2000; Rahimi-Ahar and Hatamipour, 2018; Saidi et al., 2019; Shuyan et al., 2010). In the classical SB configuration, three characteristic regions are formed, namely the spout, annulus, and fountain zones, with a cyclic flow pattern of the solids through the different regions, which contributes to enhancing the heat and mass transfer rates. The solids circulation rates are affected by the vessel's geometry and operating conditions. The insertion of a draft tube into a classical SB has been proposed to improve the SB performance for specific applications, as it enhances the system's stability and widens operating ranges by controlling the cross-flow of solids between the annulus and spout zones (Bao et al., 2013). Based on the principles of confinement of the solids in the annulus and pneumatic transport of the solids in the draft tube, some researchers suggested that this configuration could be used as a non-mechanical solids feeder to pneumatic conveying lines (Ferreira and Freire, 1992).

The fluid dynamics behavior of SB type devices operating as solids feeders to Circulating Fluidized Beds (CFBs) has been discussed by several authors (Costa et al., 2004; Ferreira and Freire, 1992; Littman and Paccione, 2015; Sousa et al., 2010). In this configuration, the SB is placed underneath the riser section of the CFB, with the riser aligned with the air inlet. The solids are stored into the SB vessel and pneumatically transported to the riser by the upward airflow. The typical solids recirculation pattern in the SB occur throughout the CFB, as the riser perform like a draft tube, and the solids return from the fountain to the feeder by the return leg.

The solids circulation rate in the CFB can be adjusted by varying the air flowrate (Q) and the distance between the air inlet and the lower end of the central tube (z). Although SB feeders have already proven to be effective to maintain stable feeding for glass beads (Geldart group D particles) under a wide range of conditions (Costa et al., 2004; Ferreira and Freire, 1992; Sousa et al., 2010), the feeder performance still needs to be assessed for biomass powders, whose characteristics and flow properties differ significantly from those of the glass beads.

Using waste biomass powders as feedstocks for producing renewable energy and fuels is appealing to reduce the dependence on fossil fuels, however, feeding reactors with these materials is still a challenge in processing (Dai et al., 2012; Ilic et al., 2018; Ramírez-Gómez, 2016). Spent Coffee Grounds (SCGs) are residues generated in huge amounts by the soluble coffee and other food industries, with recognised potential for producing thermal energy and hydrocarbon fuels (Atabani et al., 2019; Campos-Vega et al., 2015; McNutt and He, 2019; Silva et al., 1998). Depending on the powders' particle-size distribution and moisture level, SCG's flowability can be categorized from *good* to *very poor* (Massaro Sousa and Ferreira, 2019a, 2019b), hence these powders might clog mechanical feeding devices and hopper discharge orifices. Because SB feeders have a simple geometry and no moving parts, they are less expensive and suffer less wear compared to mechanical feeders. Besides, they can be used under conditions of high pressure and temperature with a reduced risk of wear and seizure. These characteristics make SB type devices a promising option for feeding waste biomass powders to reactors.

An in-depth assessment of non-mechanical feeders' performance in feeding spent coffee grounds is crucial for their successful application in CFB reactors for renewable energy generation. This paper is aimed at investigating the use of a spouted bed type device to feed SCG powders to a CFB. A comprehensive experimental study was carried out to evaluate the performance of the SB to feed dry and moist SCGs under two air flowrates (Q) and three distances between the air inlet and the bottom end of the riser (z). Two different air inlet configurations were tested, and the performance of the SB feeder was compared to results obtained using an L-valve for the same SCG powders.

2 Material and Methods

2.1 Materials

The physical and flow properties of the SCG samples are shown in Table 1. They consist of one moist sample (B_{100wet}), and two dry powders with different particle-size distributions. Samples B_{100wet} and B_{100} have a narrow particle-size distribution, from 300 and 500 μm. Sample $B_{90}C_{10}$ has a multimodal particle-size distribution, composed of 10% of particles with sizes from 150 to 300 μm, mixed with 90% of sample B_{100}. The methods used for samples' characterization are described in detail elsewhere (Massaro Sousa and Ferreira, 2019a).

These samples were chosen to evaluate the performance of the feeding system because their sizes and moisture contents match the properties of SCG powders used in the soluble coffee industry for producing thermal energy (Silva et al., 1998). Furthermore, these samples have quite different dynamic angles of repose (AoR^d), with flowability categorized from *very very poor* to *passable*, which might affect the feeding performance.

The dynamic angles of repose (AoR^d) of the samples were measured using a rotating drum with a diameter of 10 cm and a width of 4 cm, operating under the rolling flow pattern (Santos et al., 2017). The flowability classification is based on (Lumay et al., 2012; Tan et al., 2015). The minimum fluidization velocity (U_{mf}) was determined in a fluidized bed with a diameter of 0.114 m, a powder bed height of 9 cm, and with air injected uniformly at the bottom of the bed. All assays were performed in triplicate and the standard deviations are reported.

Table 1.

2.2 Experimental CFB unit with SB feeder

The experiments were carried out using the unit shown in Fig. 1a. It consists basically of a non-mechanical spouted bed feeder (1) that transports the solids stored in it to the riser (3) by adding air to the bottom inlet (2). An inclined separator (4) and a cyclone (5) collect the solids at the top of the riser and return them to the spouted bed after going through the solids' flowrate measurement system (6) and the return leg (7), thus completing the circulation loop.

The air escapes through the cyclone overflow, while the solids are kept in continuous circulation mode in the CFB by feeder's aeration. In combustion and gasification applications, SCGs react with hot gas at the riser section, and the produced gases and ashes flow out through the cyclone overflow to other process' units.

Fig. 1.

The dimensions of the cold-flow CFB are shown in Fig. 1b, with an overall height of 2 m and riser internal diameter of 0.021 m. The entire system is built of stainless steel, except for the spouted bed detailed in Fig. 1c that is made of galvanized iron with a convergent cone at the air inlet as shown in the detail. The solids circulation rate (W_S) in the CFB unit was measured using the sampler device shown in Fig. 1d. It consists of a reservoir divided by a perforated screen plate that can be moved to deviate the solids flow for sampling with minimum flow disturbance (Costa et al., 2004). The mass of collected powders was weighted in a digital balance model BG-4000 (Gehaka, São Paulo, Brazil) with an accuracy of 0.01 g.

The manometric pressures were measured at different taps located in the riser (R1 to R4), cyclone underflow (CY), return leg (RL), and air inlet (IN). The acquisition of pressure data was performed by a cDAQ-9172 chassis (National Instruments, Texas, USA) with the NI 9205 module (32-channel, +/−10 V, 250 kS/s, 16-bit analog input). The data was collected at a rate of 2500 samples/s and the mean values were recorded at every 4s.

2.3 Experimental conditions

The experiments were designed to evaluate the influence of the air flowrate (*Q*), the distance between the air inlet and the bottom end of the riser (*z*), SCG properties and air inlet configuration on the spouted bed feeder performance. The runs are summarized in Table 2 for two different values for *Q* and three values for *z*. The air inlet configuration was modified by using a convergent nozzle at the air inlet (see the detail in Fig. 1c) as an alternative to the conventional air inlet through a central orifice, also shown in the detail of Fig. 1c.

Table 2

The range of *Q* used in the assays were determined based on previous experiments with sample B_{100}. The higher limit for *Q* was set to avoid significant loss of powders at the cyclone overflow, whereas the lower limit corresponds to the minimum air flowrate that provided a stable solids flowrate in the riser. Note that pulsating unsteady transport of SCGs in this system occur at Q=38 L/min.

2.4 Experimental procedure

The experimental procedure consisted of adjusting *z* to 3, 4, or 5 cm and loading the spouted bed with 1.4 kg of SCG powder. After, the air flowrate supplied by a compressor was set to 52±2 or 62±2 L/min and inserted into the SB bottom. Every 4 s, the pressures around the CFB loop were recorded. The solids circulation rates were determined after weighing the masses collected by 10 s in the sampler. Five repetitions were carried out for each condition. The mean values for pressures and W_S under stable flow conditions are reported along with their standard deviations.

At the end of each assay, the powder that remained in the CFB unit was collected and weighted. As powder agglomeration within the system was not observed, the loss of powder in the cyclone overflow was estimated by a mass balance. The production of fine particles by attrition was determined by sifting the collected powder. The change in the powder's moisture content was also estimated by comparing the moisture content in the samples before and after the assays. It was found that the loss of powder at the cyclone overflow was less than 2% of the loaded mass. Particle-particle and particle-wall attrition were not relevant in the conditions tested, as the production of particles with sizes under 300 μm was less than 1%. The changes in the moisture content of sample B_{100wet} after the experiments were less than 4% for all conditions tested.

3 Results and Discussion

3.1 Influence of Q and z on W_S

The circulation rates for sample B_{100} under different Q and z are shown in Fig. 2. The flow was always stable and W_S fluctuated less than 20% during each experimental condition. Increasing Q and z increased W_S from 3.0 to 11.0 g/s, which might be attributed, respectively, to an increase in the gas phase momentum and to the wider area available for the solids to be dragged by the airflow into the riser as the space between the riser bottom and cone wall is enlarged. Both factors contribute to enhancing the circulation rates in the CFB. The effect of z and Q on the solid flowrates qualitatively agrees with previous studies from literature (Costa et al., 2004; Ferreira and Freire, 1992; Sousa et al., 2010).

Fig. 2.

Nevertheless, the change in Q seems to affect Ws more significantly as compared to changes in z. By increasing Q by 19% (from 52 to 62 L/min), an increase of 75% on average is observed in W_S, while increasing z by 30% (from 3 to 4 or from 4 to 5 cm) increases W_S by only 42%. These results suggest that in processing, solids circulation rates can be easily set to the desired target by adjusting Q and z. A fine-tuning in W_S values for sample B_{100} might be done by changing z.

3.2 Influence of SCG's particle-size distribution and moisture content on W_S

The circulation rates for sample B_{100wet} under different *Q* and *z* are shown in Fig. 3. The SB also provided stable feeding for the wet SCG sample, with fluctuations of *Ws* less than 20%. Considering the standard deviations, one can observe that the values of *Ws* for samples B_{100wet} and B_{100} (see Fig. 2) are similar under *Q*=52 L/min. This is because although the minimum fluidization velocity of the wet powder is higher than that of the dry one, flowability of sample B_{100wet} is better (i.e. particle-particle interactions that restrict the flow of solids are less intense), as shown in Table 1. From a practical perspective, this means that sample B_{100} can be transported more easily in the riser at *Q*=52 L/min, however, the flow of solids from the annular region of the spouted bed to the riser entrance is possibly restricted by the enhanced particle-particle interactions and fluidization effects. Therefore, similar *Ws* were verified for these samples under *Q*=52 L/min.

Fig. 3.

Nevertheless, increasing *Q* from 52 to 62 L/min had a less pronounced effect on W_S for the wet sample. SCG particles have a porosity of 14% (Massaro Sousa and Ferreira, 2019b) and water can penetrate into the internal voids, hence increasing the particle density and the hydrodynamic energy required to transport them as compared to the dry particles. This is corroborated by the higher values of U_{mf} of the wet sample (Table 1). Although additional energy is provided by increasing *Q* from 52 to 62 L/min, the increment in *Q* was insufficient to increase *Ws* significantly. Note that the ratio between mean gas velocity at the air inlet and minimum fluidization velocity for sample B_{100wet} ranged from 12.5 to 14.9, while it ranged from 17.9 to 21.3 for sample B_{100}. Therefore, W_S of sample B_{100wet} could be probably increased by using higher values for *Q* than those tested in the present study.

The effect of changing *z* is less pronounced for sample B_{100wet} (Fig. 3) compared to B_{100} (Fig. 2). As shown in Table 1, the wet sample has better flowability than the dry powder, hence the flow of particles B_{100wet} from the annular region to the riser is possibly enhanced. In turn, the effect of geometric constraints on the solids flow is weaker and for the wet sample *Ws* does not change considerably with *z*. Therefore, controlling W_S for wet samples with an SB feeder seems to be more effective by adjusting *Q* instead of *z*. Note that the term wet, in this case, refers to a water saturation level at which the liquid bridges are not strong enough to worsen the sample's flow properties (Massaro Sousa and Ferreira, 2019a).

The circulation rates of sample $B_{90}C_{10}$ under different *Q* and *z* are shown in Fig. 4. In this case, increasing *Q* increases W_S by almost four times, however, a stable operation was achieved only for a narrow range of *Q* and *z*. Besides, under the same *Q* and *z*, the circulation rates of sample $B_{90}C_{10}$ are lower than those of sample B_{100} (see Fig. 2). These feeding limitations can be explained by the poorer flowability attributes of sample $B_{90}C_{10}$, as shown in Table 1.

Fig. 4.

Continuous and steady solids feeding is essential and critical for biomass conversion processes and the feeder is usually the most problematic component of the entire reactor system (Dai et al., 2012; Ramírez-Gómez, 2016). From Sections 3.1 and 3.2, one can notice that the SB device provided stable solids feeding for dry and wet SCG powders under a wide range of conditions and could also operate with powders with different flowability attributes. Although feeding effectiveness might still be improved by assessing the influence of the SB design, the results shown here indicate that SBs are appealing devices to handle such biomass powders.

Furthermore, it is shown that the SB feeder performance is affected by the samples' properties and to ensure effective handling, the powder's flowability attributes and moisture content should be considered in the feeder's design. The previous knowledge of the powder's properties to be processed can be used to define adequate strategies to control W_S (i. e., based on either changing *Q* or *z*) and is useful information to avoid feeder's malfunction. Note that the poor flow properties of SCG powders are a consequence of their bio-based nature and processing, therefore, they are inherent of waste biomass powders.

3.3 Effect of the air inlet configuration on W_S

The circulation rates of sample B_{100} using the conventional air inlet configuration are shown in Fig. 5. The data present a wider dispersion compared to the operation with the convergent type nozzle under similar conditions (Fig. 2). Besides, considering the standard deviations, W_S remained the same regardless of the value of Q, which is a different behavior from that observed in Fig. 2. The convergent nozzle accelerates the airflow close to the riser inlet and avoids air escape to the annular region. By directing more air towards the riser, it enhances the feeders' performance. The influence of the air inlet configuration on SB feeder stability has been investigated in previous research (Sousa et al., 2010) and the use of a reduction nozzle at the air inlet is recommended to direct a major portion of the air jet into the riser.

Fig. 5.

3.4 Effect of Q and z on the pressures around the CFB loop

The pressures as a function of the height of the CFB unit are presented in Fig. 6 for sample B_{100} under different Q and z. Similar patterns are observed in all profiles, as follows: the highest and lowest pressure points are located respectively at the air inlet (IN) and close to the cyclone overflow (CY); a linear decrease in the pressure is observed at the riser section, from taps R2 to R4; and the pressure at the return leg is lower than in the riser, indicating that Q is directed mostly towards the riser.

From Fig. 2 and Fig. 6, the pressures in the feeder and riser increase as W_S rises. It means that more hydrodynamic energy is necessary to maintain the solids circulation in the CFB. The increase in the pressures is particularly evident under Q=52 L/min and z=3 and 5 cm, in which the profile of the latter z is shifted to the right in Fig. 6. The same behavior is observed when Q rises from 52 to 62 L/min with z=5 cm, however, in this case, the pressure profile of the whole CFB is shifted to the right due to the presence of more air in the system.

Fig. 6.

The pressure around the CFB loop for samples B_{100wet} and $B_{90}C_{10}$ under different Q and z are presented in Fig. 7 and Fig. 8, respectively. Similar behavior to that described for the assays with sample B_{100} can be observed here. The pressure in the feeder and in the riser are higher for the conditions of higher W_S. Therefore, in Fig. 7 and Fig. 8 the pressure profile is shifted to the right under Q=62 L/min in comparison to Q=52 L/min. Finally, the difference between the pressure values under different conditions in Fig. 7 is not as pronounced as observed in Fig. 6, because the effect of Q and z on W_S was less significant for the wet powder (see Fig. 3).

Fig. 7.

Fig. 8.

3.5 Correlations between SCG's circulation rate and pressure drop

As discussed in Section 3.4, the pressures throughout the CFB loop are linked to the solids circulation rates. It is common knowledge that in commercial units it is difficult to perform online measurements to monitor the solids flowrates. Hence, reliable correlations based on easily measurable variables might be useful and contribute to enhancing process stability, safety, automation, and performance. The manometric pressures measured at the taps IN and R1 were correlated to SCG's circulation rates, as shown in Fig. 9.

Fig. 9.

Linear equations were fitted from the experimental data accordingly:

$$P_{IN} = 53.60W_S + 167.2 \quad (1)$$

$$P_{R1} = 29.99W_S + 74.6 \quad (2)$$

A regression coefficient of 0.83 was obtained for Eqs. (1) and (2), and the experimental values differ from the estimated ones by 17% on average, which is within the standard deviations observed in W_S measurements. To improve the fitting, data obtained with sample $B_{90}C_{10}$ were not considered in Eqs. (1) and (2). The experimental data is randomly distributed around the lines of Eqs. (1) and (2), which is evidence of non-biased fittings. Therefore, the SCG's circulation rate can be accurately predicted based on pressure measurements carried out either in the feeder or in the riser. From the perspective of process control, this is an interesting result, as it suggests that W_S can be monitored throughout processing based on simple online pressure measurements.

Note that an accurate prediction of W_S with Eqs. (1) and (2) depends on whether operating conditions and equipment scale are like those investigated here. In our view, a more generalized correlation to be valid for different feeder scales and operating conditions could be proposed only after identifying the effects of some geometric parameters of equipment and powder properties on the feeder performance. Therefore, further research concerning the influence of the SB cone angle, riser diameter, particle-size distribution, and moisture content on the CFB pressure distribution and W_S would be useful.

3.6 Mean voidage in the riser

The mean voidage in the riser section (ε_r) was estimated by:

$$\Delta P_r = \rho_p(1 - \varepsilon_r)g\Delta h_r \quad (3)$$

where ΔP_r is the pressure loss in the distance Δh_r measured between taps R1 and R4.

Considering all the assays, the estimated mean voidage in the riser was equal to 0.92±0.02. Based on the air properties (ρ_{air}= 1.283 kg/m^{3,} μ_{air}=0.000018 Pa.s), particle density, and on values of Q and Ws, it was verified that the CFB riser was operated always under a dilute regime, according to the diagram proposed by Bi and Grace (Grace et al., 1997).

3.7 Comparison with a non-mechanical L-valve feeding SCGs

In a previous study, a non-mechanical L-valve (LV) has been tested to feed the SCG samples shown in Table 1 to the same CFB unit of the present study (Massaro Sousa and Ferreira, 2020). Thus, the performance of both feeders can be compared in terms of solids flowrate range, feeder's pressure drops, and flexibility to handle biomass powders with different properties. The ranges of Q, W_S and pressure drops (ΔP) in the LV and SB feeders are shown in Table 3 for samples B_{100}, B_{100wet}, and $B_{90}C_{10}$.

Table 3.

Concerning the overall performance, both feeders were easy to operate and provide reliable feeding of SCG powders into the CFB, with solids flowrate fluctuations less than 20%. Besides, the solids circulation rates could be well-correlated to simple pressure drop measurements in both cases, which is interesting from the process control point of view.

In terms of pressure drop, both feeders operated under ranges of ΔP lower than 1kPa for all the samples, which suggests that they are appealing to be used in commercial applications. However, the SB feeder showed improved performance over the LV in feeding samples B_{100} and $B_{90}C_{10}$, as it provides a wider range of W_S values under lower values of Q. An important advantage of the SB feeder is that W_S can be adjusted by two operating variables (Q and z), while in the L-valve W_S is adjusted only by the air flowrate. Thus, it is easier setting W_S to the desired targets with the SB feeder, especially for the dry samples whose flowability is poorer.

In the case of the wet sample (B_{100wet}), a wider range of W_S was obtained with the L-valve, however, as mentioned in Section 3.2, it is possible to rise Q in the SB feeder to increase the solid circulation rates of the wet sample. Thus, both feeders can be considered adequate options for handling the wet SCG powder.

Physical and flow properties of waste biomass powders might change throughout processing. An effective feeder should provide stable solids feeding, with smooth variations in

W_S even in situations in which the material's properties change. Based on our results, the SB was more flexible to handle the biomass spent coffee grounds than the L-valve. This is a relevant finding bearing in mind that L-valves have been reported to be more attractive to feed some processing powders to CFBs than other non-mechanical devices, such as the loop seal and J-valves (Cheng et al., 1998; Kim et al., 2008).

Finally, a couple of points should be highlighted concerning the implementation of SBs in commercial applications, as summarized below.

Differently than other non-mechanical feeders, with the SB the solids are stored in the feeder itself, which may have two implications: i) the handling of solids through units before the reactor might be easier with SBs, since the use of storage silos can be reduced. Consequently, the blockage of the silo's discharge orifice, which is a common drawback when operating with biomass powders, would be avoided; ii) as part of the air flowrate is inevitably dispersed towards the annulus section, it is important to consider the possibility of combustion risks in the vessel for high-temperature processes.

Some future studies aiming at improving the SB feeder performance would be useful to address: i) the effect of some SB design parameters (such as cone angle, air inlet diameter, among others), and ii) the effect of scaling-up the feeder and riser diameters on the performance. The experimental data presented here might be valuable for validation of numerical models, which can be applied to study those geometric parameters and develop scale-up rules in a cost-effective way.

4 Conclusions

The non-mechanical SB is a robust feeding device to control the circulation of dry and wet SCG powders (MC≤30% and d_{SV} close to 400 μm) in a CFB unit. The SB can be considered a more flexible alternative for continuous handling of this biomass powder residue when compared to a traditional non-mechanical L-valve. The SCG's circulation rate in the CFB was successfully controlled with the SB, with fluctuations less than 20% in *Ws*. Besides, W_S could be easily set to desired targets by adjusting Q and z, and it can be monitored by simple pressure measurements in the feeder or in the riser as well. We verified that solids' feeding is more stable by using a convergent nozzle at the air inlet instead of using a conventional orifice air inlet. Also, feeding performance is affected by the powder attributes, thus the samples' flowability properties and moisture level should be considered in designing spouted bed feeders. These findings might be useful to engineers and technicians interested in implementing continuous and effective feeding of SCGs to reactors for renewable energy generation and for fuel production based on biomass residues.

Acknowledgements

The authors would like to thank the São Paulo Research Foundation (2016/25946-2 and 2018/11031-8), and CAPES (Finance code 001) for financial support.

Nomenclature

AoR^d	Dynamic angle of repose (°)
D	Riser diameter (mm)
d_{SV}	Sieve mean diameter (μm)
g	Gravitational constant ($m \cdot s^{-2}$)
H	Riser height (m)
MC	Moisture content (% wet basis)
P_{IN}	Manometric pressure measured at tap IN (Pa)
P_{R1}	Manometric pressure measured at tap R1 (Pa)
Q	Air flowrate ($L \cdot min^{-1}$)
U_{mf}	Minimum fluidization velocity ($m \cdot s^{-1}$)
Ws	Solids flowrate ($g \cdot s^{-1}$)
z	
Greek symbols	
Δh_r	Distance between taps R1 and R4 (m)
ΔP	Feeders' pressure drop (Pa)
ΔPr	Pressure drop in the riser (Pa)
ε_r	Mean voidage in the riser (-)
μ_{air}	Viscosity of the air ($Pa \cdot s$)

ρ_{air}	Air density (kg·m^{-3})
ρ_p	Particle density (kg·m^{-3})

References

Atabani, A.E., Al-Muhtaseb, A.H., Kumar, G., Saratale, G.D., Aslam, M., Khan, H.A., Said, Z., Mahmoud, E., 2019. Valorization of spent coffee grounds into biofuels and value-added products: Pathway towards integrated bio-refinery. Fuel 254, 1–20.

Bao, X., Du, W., Xu, J., 2013. An overview on the recent advances in computational fluid dynamics simulation of spouted beds. Can. J. Chem. Eng. 91, 1822–1836.

Campos-Vega, R., Loarca-Piña, G., Vergara-Castañeda, H.A., Oomah, B.D., 2015. Spent coffee grounds: a review on current research and future prospects. Trends Food Sci. Technol. 45, 24–36.

Cheng, Y., Fei, W., Yang, G., Yong, J., 1998. Inlet and outlet effects on flow patterns in gas-solid risers. Powder Technol. 98, 151–156.

Costa, I.A., Ferreira, M.C., Freire, J.T., 2004. Analysis of regime transitions and flow instabilities in vertical conveying of coarse particles using different solids feeding systems. Can. J. Chem. Eng. 82, 48–59.

Cui, H., Grace, J.R., 2008. Spouting of biomass particles: A review. Bioresour. Technol. 99, 4008–4020.

Dai, J., Cui, H., Grace, J.R., 2012. Biomass feeding for thermochemical reactors. Prog. Energy Combust. Sci. 38, 716–736.

Ferreira, M.C., Freire, J.T., 1992. Fluid Dynamics Characterization of a Pneumatic Bed Using a Spouted Bed Type Solid Feeding System. Can. J. Chem. Eng. 70, 905–909.

Grace, J.R., Avidan, A.A., Knowlton, T.M., 1997. Circulating Fluidized Beds, 1st ed, Principles of Gas–Solid Flows. Chapman & Hall.

Ilic, D., Williams, K., Farnish, R., Webb, E., Liu, G., 2018. On the challenges facing the handling of solid biomass feedstocks. Biofuels, Bioprod. Biorefining 12, 187–202.

Jono, K., Ichikawa, H., Miyamoto, M., Fukumori, Y., 2000. A review of particulate design for pharmaceutical powders and their production by spouted bed coating. Powder Technol. 113, 269–277.

Kim, J., Tachino, R., Tsutsumi, A., 2008. Effects of solids feeder and riser exit configuration on establishing high density circulating fluidized beds. Powder Technol 187, 37–45.

Littman, H., Paccione, J.D., 2015. New Type of Draft Tube Spout-Fluid Bed. Part 2: Modeling and Design of the Acceleration Section of the Riser for the Pneumatic Transport of 1 mm Glass Spheres. Ind. Eng. Chem. Res. 54, 6187–6198.

Lumay, G., Boschini, F., Traina, K., Bontempi, S., Remy, J.C., Cloots, R., Vandewalle, N., 2012. Measuring the flowing properties of powders and grains. Powder Technol. 224, 19–27.

Massaro Sousa, L., Ferreira, M.C., 2020. Analysis of the Performance of an L-Valve Feeding Spent Coffee Ground Powders into a Circulating Fluidized Bed. Powder Technol. 362, 759–769.

Massaro Sousa, L., Ferreira, M.C., 2019a. Spent coffee grounds as a renewable source of energy: An analysis of bulk powder flowability. Particuology 43, 92–100.

Massaro Sousa, L., Ferreira, M.C., 2019b. Densification behavior of dry spent coffee ground powders: Experimental analysis and predictive methods. Powder Technol. 357, 149–157.

Mathur, K.B., Gishler, P.E., 1955. A technique for contacting gases with coarse solid particles. AIChE J. 1, 157–164.

McNutt, J., He, Q., 2019. Spent coffee grounds: A review on current utilization. J. Ind. Eng. Chem. 71, 78–88.

Rahimi-Ahar, Z., Hatamipour, M.S., 2018. Hydrodynamics, numerical study and application of spouted bed. Rev. Chem. Eng. 34, 743–766.

Ramírez-Gómez, A., 2016. Research needs on biomass characterization to prevent handling problems and hazards in industry. Part. Sci. Technol. 34, 432–441.

Saidi, M., Basirat Tabrizi, H., Grace, J.R., 2019. A review on pulsed flow in gas-solid fluidized beds and spouted beds: Recent work and future outlook. Adv. Powder Technol. 30, 1121–1130.

Santos, L.C., Condotta, R., Ferreira, M.C., 2017. Flow properties of coarse and fine sugar powders. J. Food Process Eng. 41, 1–10.

Shuyan, W., Zhenghua, H., Dan, S., Yikun, L., Lixin, W., Shuai, W., 2010. Hydrodynamic simulations of gas-solid spouted bed with a draft tube. Chem. Eng. Sci. 65, 1322–1333.

Silva, M.A., Nebra, S.A., Machado Silva, M.J., Sanchez, C.G., 1998. The use of biomass residues in the Brazilian soluble coffee industry. Biomass and Bioenergy 14, 457–467.

Sousa, R.C., de Almeida, A.R.F., Ferreira, M.C., Freire, J.T., 2010. Analysis of fluid dynamics and thermal behavior using a vertical conveyor with a spouted bed feeder. Dry. Technol. 28, 1277–1287.

Tan, G., Morton, D.A. V., Larson, I., 2015. On the methods to measure powder flow. Curr. Pharm. Des. 21, 5751–5765.

List of Figures

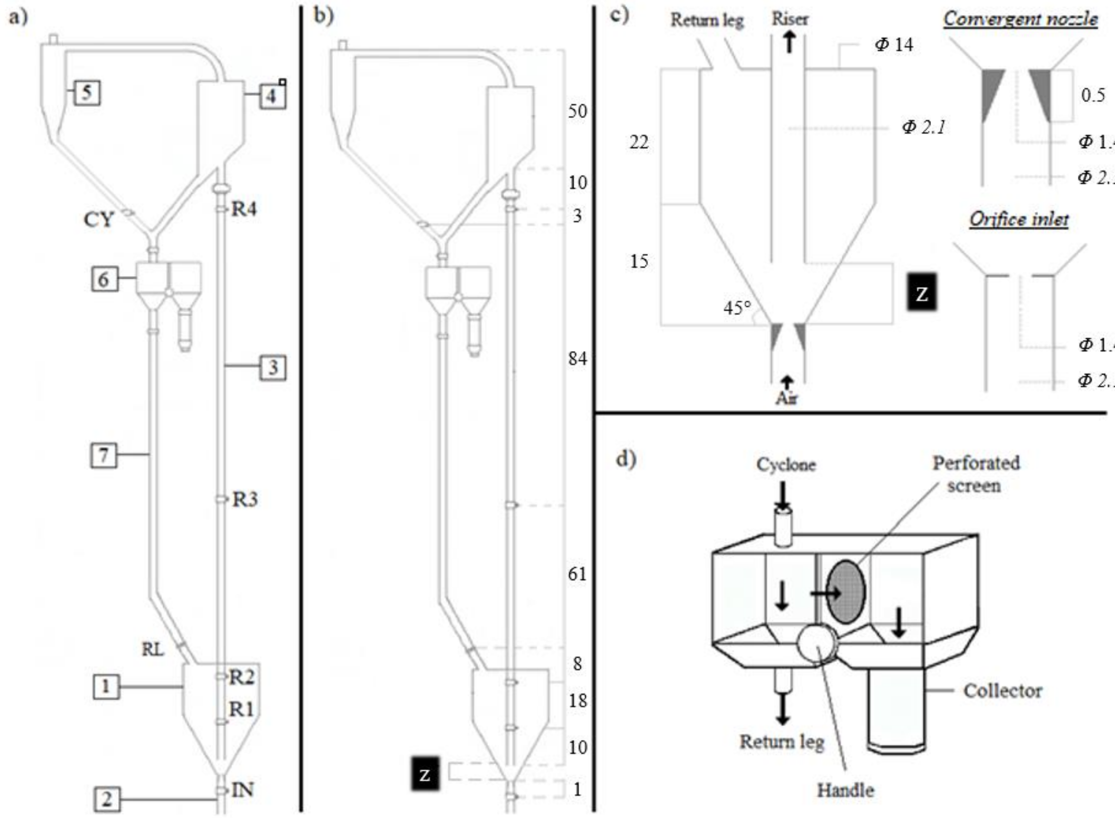

Fig. 1. CFB experimental setup. a) Main components and pressure tap positions: IN, R1 to R4, CY, and RL. b) Dimensions of the CFB unit. c) Components of the spouted bed feeder and details of the air inlet configurations. d) Solids' flowrate measurement system. All dimensions in cm.

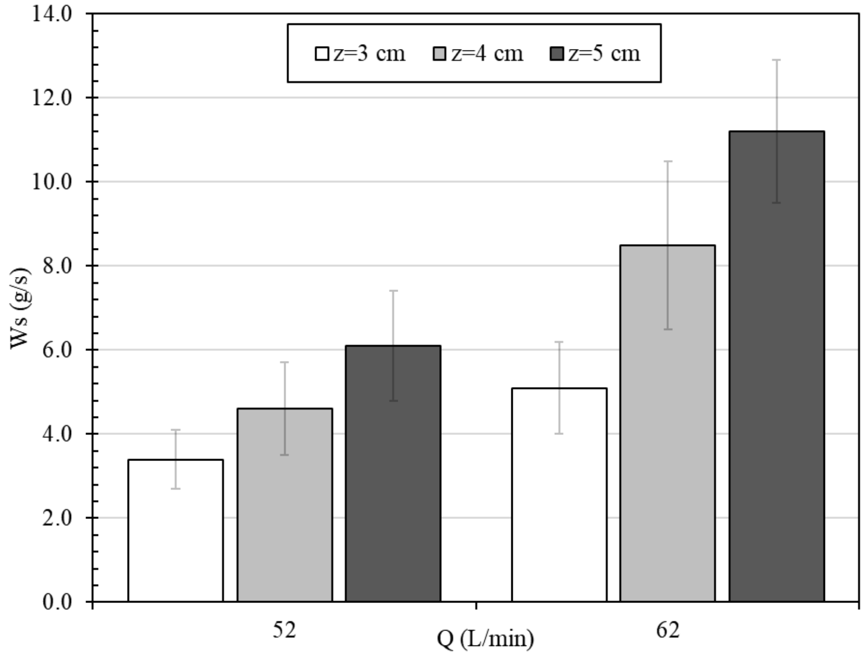

Fig. 2. Solids circulation rates for sample B_{100} under different Q and z and operation with the convergent nozzle at the air inlet.

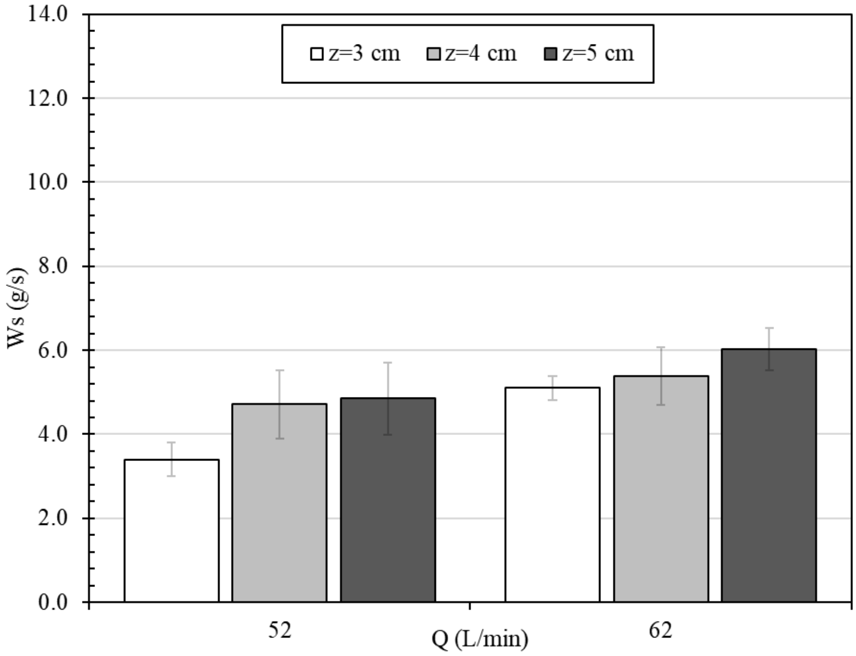

Fig. 3. Solids circulation rates for sample B_{100wet} under different values of *Q* and *z*.

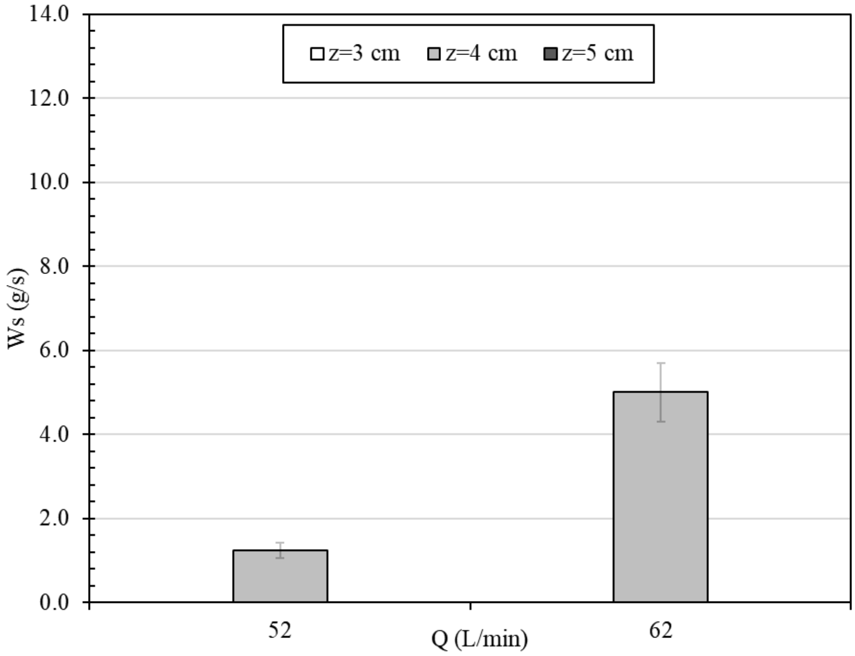

Fig. 4. Solids circulation rates of sample $B_{90}C_{10}$ under different values of *Q* and *z*.

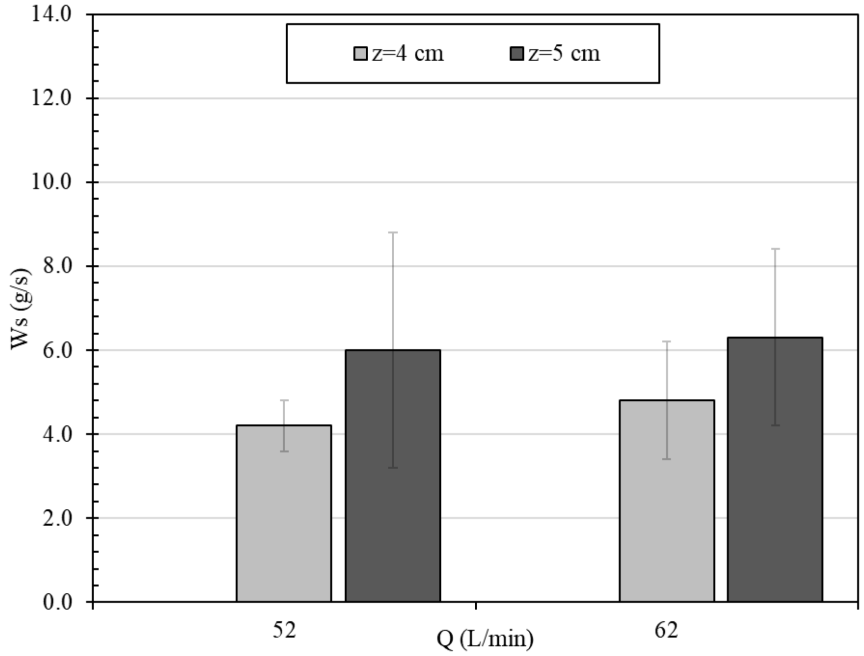

Fig. 5. Solids circulation rates of sample B_{100} using the conventional air inlet configuration.

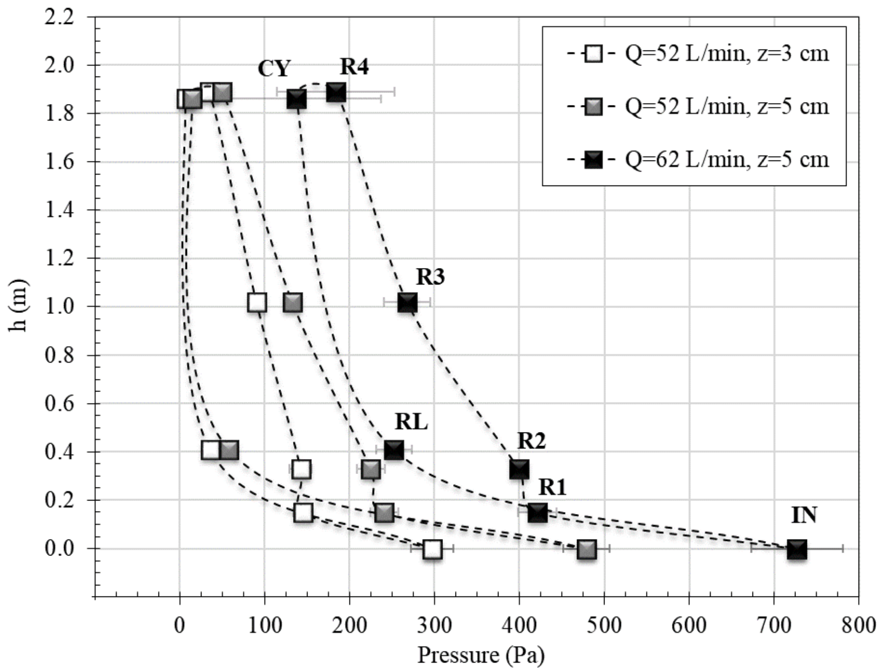

Fig. 6. Pressures around the CFB loop for sample B_{100} under different values of Q and z.

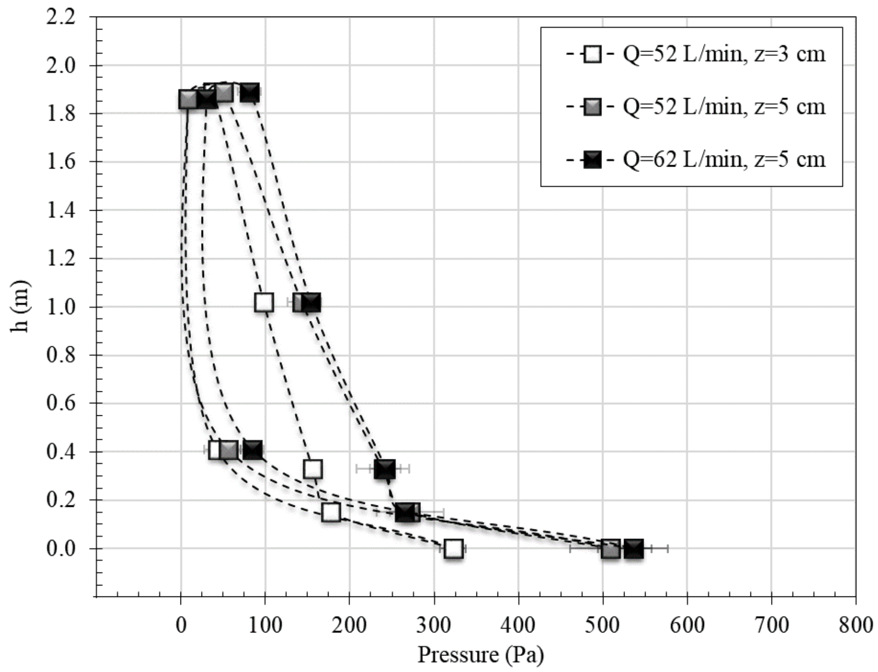

Fig. 7. Pressures around the CFB loop for sample B_{100wet} under different values of *Q* and *z*.

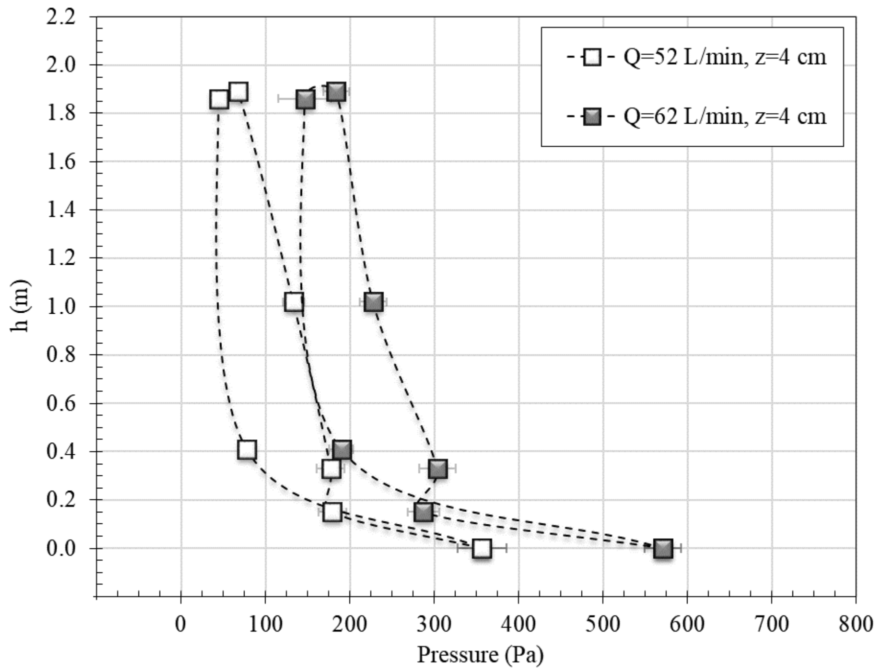

Fig. 8. Pressures around the CFB loop for sample $B_{90}C_{10}$ under different values of *Q* and *z*.

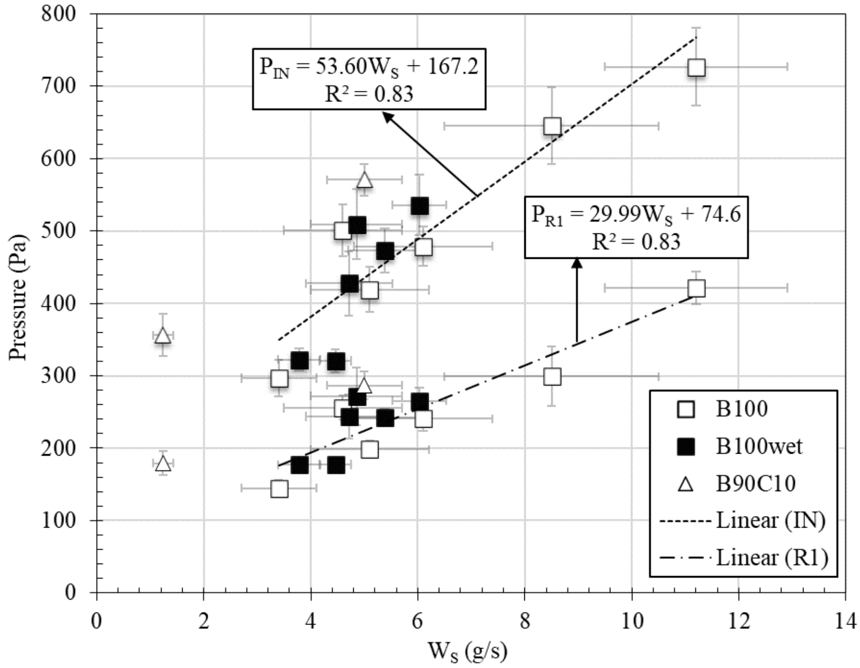

Fig. 9. Manometric pressures measured at the air inlet (P_{IN}) and riser inlet (P_{R1}) versus solids circulation rate.

List of Tables

Table 1. Physical and flow properties of the SCG samples.

SCG sample	d_{SV} **(μm)**	**MC (% w.b.)**	U_{mf} **(m/s)**	ρ_p **(kg/m³)**	AoR^d **(˚)**	**Flowability classification**
B_{100wet}	400	30.0 ± 0.3^a	0.20 ± 0.01^a	-	42 ± 2^a	Passable
B_{100}	400	2.8 ± 0.1^b	0.14 ± 0.01^b	1120 ± 20^a	62 ± 3^b	Very Poor
$B_{90}C_{10}$	370	3.2 ± 0.1^b	0.15 ± 0.01^b	1120 ± 10^a	70 ± 3^c	Very Very Poor

Values with different letters in the same column are significantly different at a 0.05 significance level.

Table 2. Summary of the experimental conditions.

Runs	**SCG sample**	***z*** **(cm)**	***Q*** **(L/min)**	**Air inlet configuration (-)**
Number 1	B_{100}	3	52	Convergent Nozzle
No. 2	B_{100}	4	52	Conv. Nozzle
No. 3	B_{100}	5	52	Conv. Nozzle
No. 4	B_{100}	3	62	Conv. Nozzle
No. 5	B_{100}	4	62	Conv. Nozzle
No. 6	B_{100}	5	62	Conv. Nozzle
No. 7	B_{100wet}	3	52	Conv. Nozzle
No. 8	B_{100wet}	4	52	Conv. Nozzle
No. 9	B_{100wet}	5	52	Conv. Nozzle
No. 10	B_{100wet}	3	62	Conv. Nozzle
No. 11	B_{100wet}	4	62	Conv. Nozzle
No. 12	B_{100wet}	5	62	Conv. Nozzle
No. 13	$B_{90}C_{10}$	3	52	Conv. Nozzle
No. 14	$B_{90}C_{10}$	4	52	Conv. Nozzle
No. 15	$B_{90}C_{10}$	5	52	Conv. Nozzle
No. 16	$B_{90}C_{10}$	3	62	Conv. Nozzle
No. 17	$B_{90}C_{10}$	4	62	Conv. Nozzle
No. 18	$B_{90}C_{10}$	5	62	Conv. Nozzle
No. 19	B_{100}	4	52	Orifice
No. 20	B_{100}	5	52	Orifice
No. 21	B_{100}	4	62	Orifice
No. 22	B_{100}	5	62	Orifice

Table 3. Ranges for air flowrate, solids circulation rate, and feeders' pressure drop in handling SCG powders.

Sample	***Q*** **(L/min)**[*]		***W**$_S$* **(g/s)**		***ΔP*** **(Pa)**	
	LV	SB	LV	SB	LV	SB
B_{100wet}	230 - 250	52 – 62	1.2 - 10.0	3.8 - 6.0	210 – 960	320 - 540
B_{100}	230 - 310	52 – 62	1.7 - 3.8	3.0 - 11.0	230 – 480	300 - 730
$B_{90}C_{10}$	235 - 270	52 – 62	0.6 - 0.7	1.2 - 5.0	110 – 130	360 - 570

[*]For the L-valve, *Q* is the sum of the aeration and riser inlet air flowrates.